

## LETTER TO THE EDITOR

## High-pressure effect on the electronic state in CeNiGe<sub>3</sub>: pressure-induced superconductivity

M Nakashima<sup>1,5</sup>, K Tabata<sup>2</sup>, A Thamizhavel<sup>1</sup>, T C Kobayashi<sup>3</sup>, M Hedo<sup>4</sup>, Y Uwatoko<sup>4</sup>, K Shimizu<sup>2</sup>, R Settai<sup>1</sup> and Y Ōnuki<sup>1</sup>

<sup>1</sup> Graduate School of Science, Osaka University, Toyonaka, Osaka 560-0043, Japan

<sup>2</sup> Research Center for Materials Science at Extreme Conditions, Osaka University, Toyonaka, Osaka 560-8531, Japan

<sup>3</sup> Department of Physics, Faculty of Science, Okayama University, Tsushimanaka, Okayama 700-8530, Japan

<sup>4</sup> Institute for Solid State Physics, University of Tokyo, Kashiwa, Chiba 277-8581, Japan

E-mail: mnaka@crystal.phys.sci.osaka-u.ac.jp

Received 5 February 2004

Published 7 May 2004

Online at [stacks.iop.org/JPhysCM/16/L255](http://stacks.iop.org/JPhysCM/16/L255)

DOI: 10.1088/0953-8984/16/20/L01

### Abstract

We have measured the electrical resistivity of an antiferromagnetic Kondo compound CeNiGe<sub>3</sub> under pressure. The Néel temperature initially increases with pressure  $P$  up to 3 GPa, then decreases rather steeply with further increasing pressure, and becomes zero at a critical pressure  $P_c \simeq 5.5$  GPa. The  $A$  and  $\rho_0$  values of the resistivity  $\rho = \rho_0 + AT^2$  in the Fermi liquid relation become maximum around  $P_c$ , the  $A$  value attaining an extremely large value which is comparable with that in a heavy fermion superconductor CeCu<sub>2</sub>Si<sub>2</sub>. Superconductivity is found below 0.48 K in a wide pressure region from 4 to 10 GPa. The upper critical field  $H_{c2}(0)$  is about 2 T, indicating heavy fermion superconductivity.

In cerium and uranium compounds, the Ruderman–Kittel–Kasuya–Yosida (RKKY) interaction and the Kondo effect compete with each other [1, 2]. The competition between the RKKY interaction and the Kondo effect was discussed by Doniach [3] as a function of  $|J_{cf}|D(\varepsilon_F)$ , where  $|J_{cf}|$  is the magnitude of the magnetic exchange interaction and  $D(\varepsilon_F)$  is the electronic density of states at the Fermi energy  $\varepsilon_F$ . Most cerium compounds order magnetically when the RKKY interaction overcomes the Kondo effect at low temperatures. The magnetic ordering is formed by the localized-4f moments of Ce<sup>3+</sup>. The topology of the Fermi surface for the conduction electrons is therefore quite similar to that of the corresponding non-4f lanthanum compounds, although the cyclotron mass of the cerium compounds is typically one to two orders of magnitude larger than that of the lanthanum compounds.

<sup>5</sup> Author to whom any correspondence should be addressed.

On the other hand, some cerium compounds such as  $\text{CeCu}_6$  and  $\text{CeRu}_2\text{Si}_2$  show no long-range magnetic ordering, because the Kondo effect overcomes the RKKY interaction. These compounds are called heavy fermion compounds since they have an extremely large electronic specific heat coefficient  $\gamma$ :  $\gamma \simeq 10^4/T_K$  ( $\text{mJ K}^{-2} \text{mol}^{-1}$ ), where  $T_K$  is called the Kondo temperature:  $T_K = 5$  K in  $\text{CeCu}_6$ , for example [1, 2]. In fact, a large cyclotron effective mass of  $120 m_0$  was detected in the de Haas–van Alphen oscillation in  $\text{CeRu}_2\text{Si}_2$  [4]. Moreover, the topology of the Fermi surface in  $\text{CeRu}_2\text{Si}_2$  is well explained by the 4f-itinerant band model, although the cyclotron effective mass is much larger than the corresponding band mass.

Recently a new aspect of cerium and uranium compounds with magnetic ordering has been discovered. When pressure  $P$  is applied to the cerium compounds with antiferromagnetic ordering such as  $\text{CeIn}_3$  and  $\text{CePd}_2\text{Si}_2$  [5], the Néel temperature  $T_N$  decreases, and a quantum critical point corresponding to the extrapolation  $T_N \rightarrow 0$  is reached at  $P = P_c$ . Here,  $|J_{\text{cf}}|D(\varepsilon_F)$  in the Doniach model can be replaced by pressure. Surprisingly, superconductivity appears around  $P_c$ . Moreover, a heavy fermion state is formed around  $P_c$ , where the non-Fermi liquid nature is also found in some compounds. Similar pressure-induced superconductivity was reported in  $\text{CeRh}_2\text{Si}_2$  [6],  $\text{CeRhIn}_5$  [7] and  $\text{UGe}_2$  [8].

The crossover from the magnetically ordered state to the non-magnetic state under pressure, crossing the quantum critical point, is the most interesting issue in strongly correlated f-electron systems. We have continued studying the effect of pressure on the cerium and uranium compounds [9]. We report in the present work a change of the electronic states in an antiferromagnet  $\text{CeNiGe}_3$ , which is tuned by high pressures up to 10 GPa. The antiferromagnetic Kondo state is changed into the heavy fermion state around a critical pressure  $P_c \simeq 5.5$  GPa and becomes a non-magnetic Fermi liquid above  $P_c$ . We have found superconductivity around  $P_c$ .

There are several intermetallic compounds in the Ce–Ni–Ge system [10–12]:  $\text{Ce}_3\text{Ni}_2\text{Ge}_7$  (a Néel temperature  $T_N = 7.2$  K),  $\text{Ce}_3\text{NiGe}_2$  ( $T_N = 6.2$  K),  $\text{CeNiGe}_3$  ( $T_N = 5.5$  K) and  $\text{Ce}_2\text{Ni}_3\text{Ge}_5$  ( $T_N = 4.8$  K). Among them, the magnetic and electrical properties of  $\text{CeNiGe}_3$  was recently clarified from electrical resistivity, magnetic susceptibility, magnetization, specific heat, neutron powder diffraction and electron diffraction experiments [11, 12]. The crystal structure is the orthorhombic  $\text{SmNiGe}_3$ -type structure ( $Cmmm$  space group, no. 65), as shown in figure 1. The lattice parameter along the  $a$ -axis is extremely large compared to those along the  $b$ - and  $c$ -axes:  $a = 21.808$  Å,  $b = 4.135$  Å and  $c = 4.168$  Å.

The magnetic susceptibility of a polycrystal sample follows the Curie–Weiss law with an effective moment  $\mu_{\text{eff}} = 2.58 \mu_B/\text{Ce}$  and the paramagnetic Curie temperature  $\theta_p = -12$  K. The effective moment is in good agreement with the theoretical value of  $\text{Ce}^{3+}$ ,  $2.54 \mu_B/\text{Ce}$ . The magnetic susceptibility has a maximum at 5.5 K and decreases with decreasing the temperature, indicating a Néel temperature  $T_N = 5.5$  K. The corresponding peak in the specific heat appears at  $T_N$ . The magnetic entropy at  $T_N$  is estimated as  $0.65R \ln 2$ , indicating a doublet ground state of the localized 4f-crystalline electric field (CEF) scheme. The electronic specific heat coefficient  $\gamma$  is obtained as  $34 \text{ mJ K}^{-2} \text{mol}^{-1}$ . The electrical resistivity decreases below the Néel temperature.

On the other hand, the neutron powder diffraction experiment indicates a complicated magnetic structure. Two magnetic transitions were observed at  $T'_N = 5.9$  K and  $T''_N = 5.0$  K.  $T'_N$  is associated with a commensurate collinear antiferromagnetic structure with a propagation vector  $\mathbf{k}_1 = (100)$ , as indicated by arrows in figure 1. The magnetic moments are oriented along the  $b$ -axis. On the other hand,  $T''_N$  is associated with an incommensurate antiferromagnetic structure with a propagation vector  $\mathbf{k}_2 = (0.409 \ 1/2)$ . Below  $T''_N$ , the two magnetic structures coexist but the incommensurate structure is highly preponderant. The magnetic moment at the Ce site is determined as  $0.8 \mu_B/\text{Ce}$  at 1.5 K.

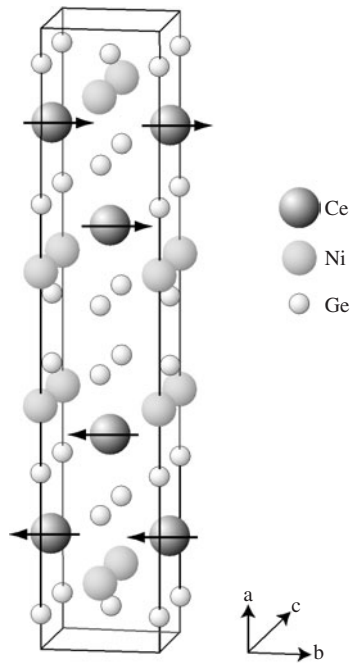


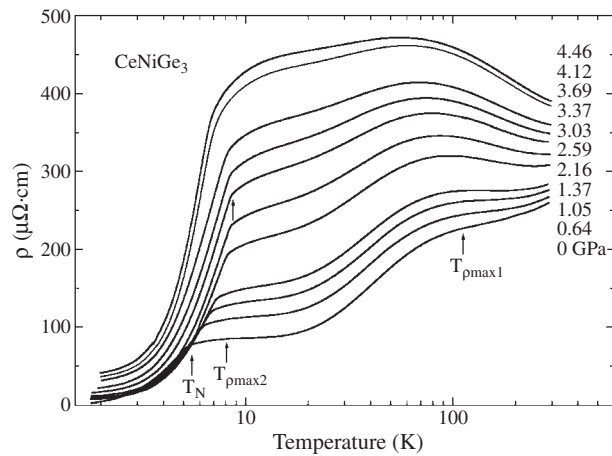
**Figure 1.** Crystal structure of  $\text{CeNiGe}_3$ . Arrows indicate the magnetic moments corresponding to the propagation vector  $k_1 = (100)$ .

The present pressure experiments on the electrical resistivity of  $\text{CeNiGe}_3$  were done by three methods. One is due to an indenter cell in the pressure range from ambient pressure to about 4 GPa in the temperature range from 2 to 300 K. Another is due to a cubic anvil cell at higher pressures up to 8 GPa in the temperature range from 2 to 300 K. The third method is due to a diamond anvil cell at pressures up to 10 GPa in the temperature range from 0.1 to 300 K. The electronic states are tuned by pressure from the antiferromagnetic state to the non-magnetic state, crossing the heavy fermion state in the critical pressure region around 5–6 GPa.

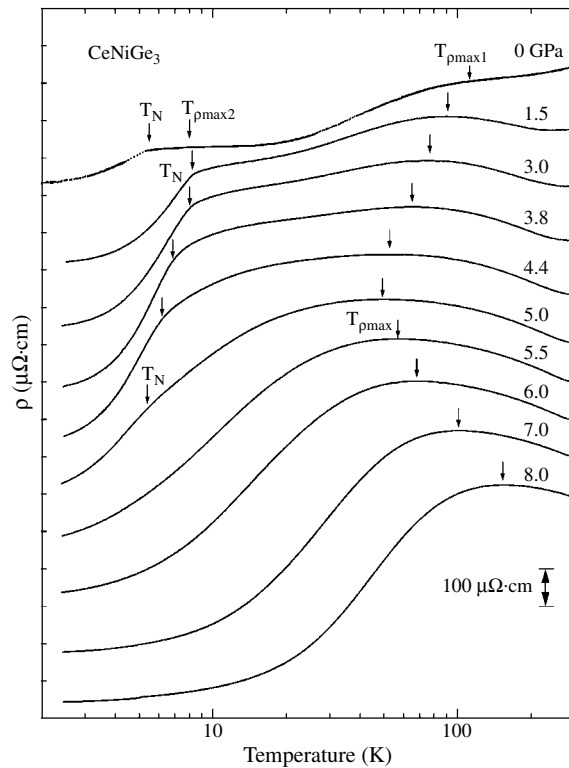
The sample was prepared by arc-melting the stoichiometric amounts of the elements with 3N-(99.9% pure) Ce, 4N-Ni and 5N-Ge under argon atmosphere. The alloy button was wrapped in a Ta-foil, sealed in an evacuated quartz tube and annealed at 800 °C for four days. The residual resistivity  $\rho_0$  and residual resistivity ratio  $\text{RRR} = \rho_{\text{RT}}/\rho_0$  were  $1.5 \mu\Omega \text{ cm}$  and 220, respectively, indicating a high-quality sample. There are no reports on a single crystal sample of  $\text{CeNiGe}_3$ . We tried to grow a single crystal by the Czochralsky method in a tetra-arc furnace but did not succeed.  $\text{CeNiGe}_3$  is believed to be an incongruently melting compound.

Figure 2 shows the logarithmic scale of temperature dependence of the electrical resistivity  $\rho$  at various pressures, which was obtained by using the indenter cell. The electrical resistivity at ambient pressure has a broad hump around 100 K and also a broad peak around 8 K, and decreases steeply below  $T_N = 5.5$  K, which are the same as the previous data [13]. These are characteristic features in the cerium Kondo compound with antiferromagnetic ordering. In cerium Kondo compounds, there are two characteristic Kondo temperatures  $T_K^{\text{h}}$  and  $T_K$  [14]. For  $\text{CeNiGe}_3$ ,  $T_K^{\text{h}}$  most likely corresponds to the temperature of 100 K showing the hump, which is named here  $T_{\rho_{\text{max1}}} = 100$  K, and shown by an arrow in figure 2.  $T_K$  roughly corresponds to 8 K, although  $\text{CeNiGe}_3$  orders antiferromagnetically below  $T_N = 5.5$  K. We define the temperature showing the broad resistivity peak as  $T_{\rho_{\text{max2}}} = 8$  K, as shown by an arrow in figure 2.

With increasing pressure, the electrical resistivity increases in magnitude, and  $T_{\rho_{\text{max1}}}$  shifts to lower temperatures, while  $T_{\rho_{\text{max2}}}$  increases with increasing pressure, as shown in figure 2.



**Figure 2.** Logarithmic scale of temperature dependence of the electrical resistivity under pressures in CeNiGe<sub>3</sub>, which was obtained by using the indenter cell. Characteristic temperatures  $T_N$ ,  $T_{\rho_{\max 1}}$  and  $T_{\rho_{\max 2}}$  are described in the text.



**Figure 3.** Logarithmic scale of temperature dependence of the electrical resistivity under pressures in CeNiGe<sub>3</sub>, which was obtained by using the cubic anvil cell.

It is, however, difficult to define  $T_{\rho_{\max 2}}$  above 1 GPa. On the other hand, the Néel temperature increases from  $T_N = 5.5$  K at ambient pressure to 8.5 K at 3.03 GPa, as shown by an arrow in figure 2, but decreases with further increasing pressure.

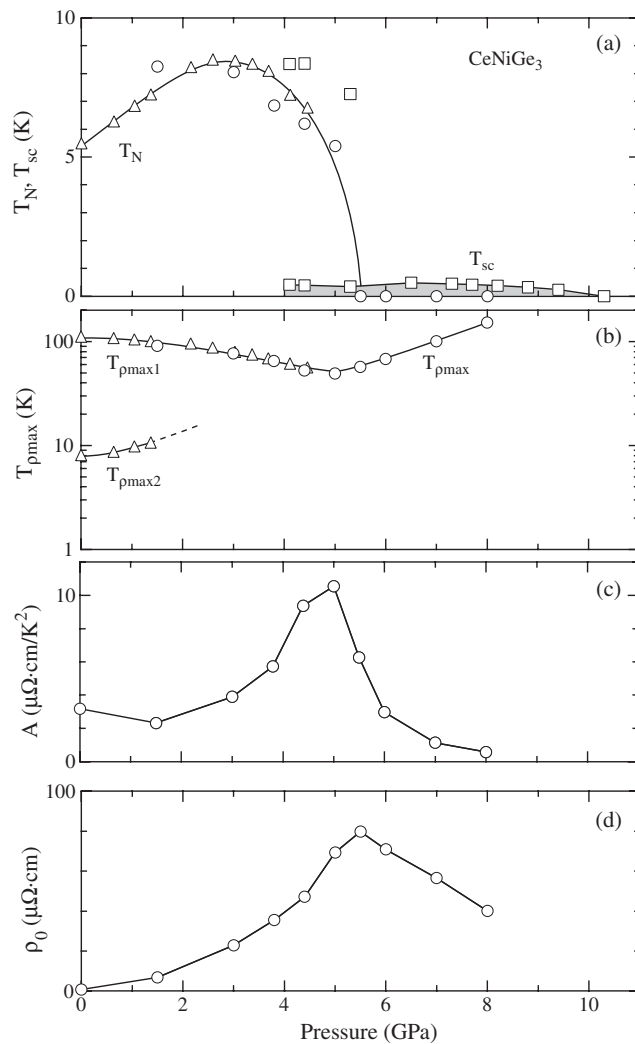


**Figure 4.** Pressure dependence of  $T_N$ ,  $T_{sc}$ ,  $T_{\rho_{max}}$ ,  $A$  and  $\rho_0$  values in  $CeNiGe_3$ . The data shown by triangles, circles and squares were obtained by the indenter, cubic and diamond anvil cells, respectively.

To clarify the behaviour of resistivity at higher pressures, we show in figure 3 the logarithmic scale of temperature dependence of the electrical resistivity at pressures up to 8.0 GPa, which was obtained by using the cubic anvil cell. The resistivity data at different pressures are arbitrarily shifted downwards for simplicity. The two characteristic features at  $T_{\rho_{max1}}$  and  $T_{\rho_{max2}}$  are found to merge at 5 GPa into a single resistivity peak at  $T_{\rho_{max}} = 50$  K. This single resistivity peak at 5 GPa shifts to higher temperatures with further increasing pressure:  $T_{\rho_{max}} = 153$  K at 8.0 GPa. The antiferromagnetic ordering most likely disappears at 5.5 GPa. The overall temperature dependence of the electrical resistivity around 5–6 GPa is very similar to that in a heavy fermion superconductor  $CeCu_2Si_2$  [15]. On the other hand, the electrical resistivity at 8.0 GPa is typically similar to that observed in a valence fluctuating compound such as  $CeNi$ , where the 4f electron is itinerant [16].

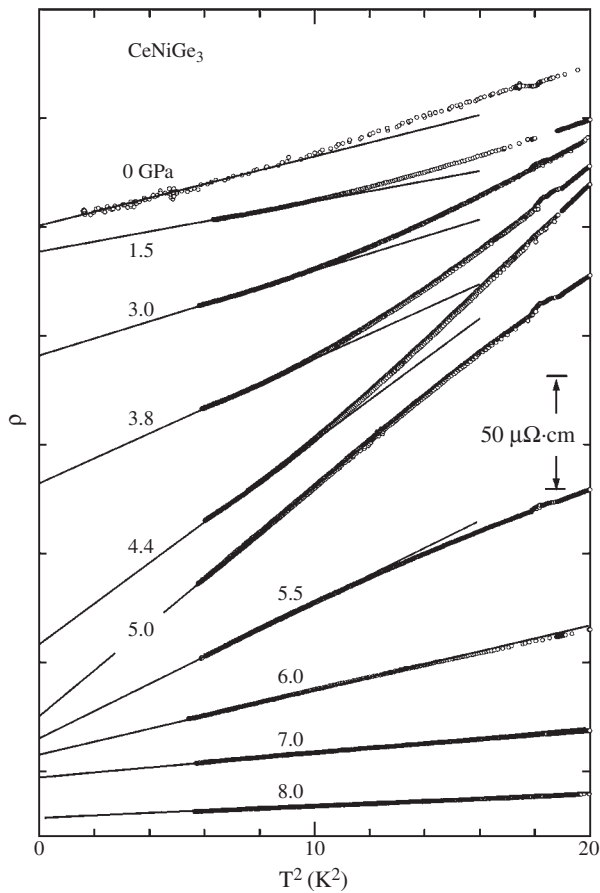


**Figure 5.**  $T^2$ -dependence of the electrical resistivity of CeNiGe<sub>3</sub>.

Figure 4(a) shows the pressure dependence of the Néel temperature  $T_N$ . The data shown by triangles, circles and squares were obtained by using the indenter, cubic and diamond anvil cells, respectively. The data obtained by the diamond anvil cell measurement are described later. Solid lines connecting the data are guidelines. As mentioned above, the Néel temperature attains a maximum at 3 GPa, decreases rather steeply at higher pressures and becomes zero at  $P_c \simeq 5.5$  GPa. The two characteristic temperatures  $T_{\rho_{\max 1}}$  and  $T_{\rho_{\max 2}}$  merge into a single characteristic temperature  $T_{\rho_{\max}}$  above 5 GPa, as shown in figure 4(b).

Here we tried to obtain the  $A$  and  $\rho_0$  values from the  $T^2$ -dependence of the electrical resistivity at low temperatures, following a Fermi liquid relation, as shown in figure 5. The resistivity data, which were obtained by using the cubic anvil cell, are arbitrarily shifted. Solid lines represent the  $\rho = \rho_0 + AT^2$  relation. The  $A$  value, which corresponds to the slope of the solid line, becomes maximum around  $P_c \simeq 5.5$  GPa, as shown in figures 5 and 4(c). The  $A$  value at 5 GPa,  $10.5 \mu\Omega \text{ cm K}^{-2}$  is the same as  $10 \mu\Omega \text{ cm K}^{-2}$  in a heavy fermion superconductor CeCu<sub>2</sub>Si<sub>2</sub> with an extremely large  $\gamma$  value of  $1.1 \text{ J K}^{-2} \text{ mol}^{-1}$  [15]. The heavy fermion state is thus formed around  $P_c \simeq 5.5$  GPa. Correspondingly, the residual resistivity  $\rho_0$  value also becomes maximum around  $P_c \simeq 5.5$  GPa, as shown in figure 4(d).

In order to look for possible superconductivity around  $P_c$ , we measured the low-temperature resistivity. Figure 6 shows the temperature dependence of the electrical resistivity at 6.5 GPa under several magnetic fields, which was obtained by using the diamond anvil cell.

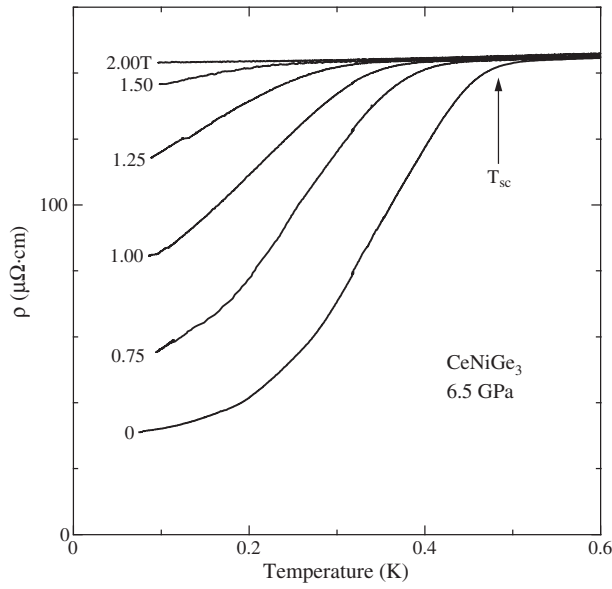


**Figure 6.** Low-temperature resistivity at 6.5 GPa under several magnetic fields in CeNiGe<sub>3</sub>.

At zero field, the resistivity decreases rather slowly below 0.5 K. With increasing magnetic fields, the onset of the resistivity drop shifts to lower temperatures and vanishes at  $H = 2.00$  T. These results indicate that the present resistivity drop is due to superconductivity.  $H_{c2}(0) \simeq 2$  T is consistent with  $H_{c2}(0) = 2.0\text{--}2.4$  T in CeCu<sub>2</sub>Si<sub>2</sub> [15], together with the  $A$  value mentioned above.

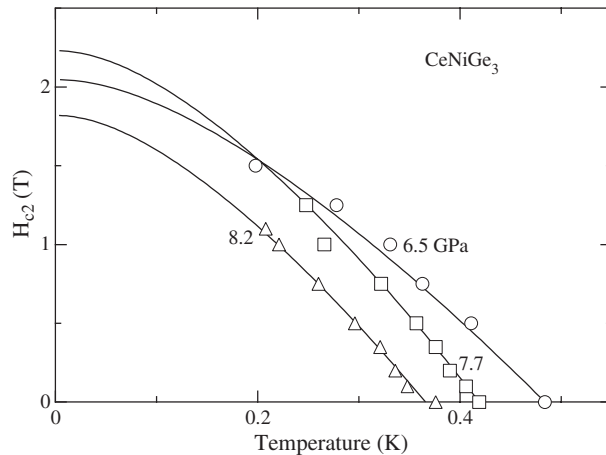
We define here the superconducting transition temperature  $T_{sc}$  as the onset of the resistivity drop, which is defined as the temperature showing a minimum of  $d^2\rho/dT^2$ , for example,  $T_{sc} = 0.48$  K at zero field, as shown by an arrow in figure 6.

Figure 7 shows the temperature dependence of the upper critical field  $H_{c2}$  at three pressures. The solid curves are guidelines based on the WHH theory [17].  $H_{c2}(0)$  at 6.5 GPa is roughly estimated as 2.0 T, indicating a coherence length  $\xi = 130$  Å from  $H_{c2} = \phi_0/2\pi\xi^2$ , where  $\phi_0$  is the quantum fluxoid.

We also show in figure 4(a) the pressure dependence of the Néel temperature  $T_N$  and the superconducting transition temperature  $T_{sc}$  by squares. Superconductivity is observed in a wide pressure region from 4 to 10 GPa in the diamond anvil cell experiment. We note here that the Néel temperature shown by squares is shifted to a higher pressure by about 1 GPa compared to that shown by triangles and circles. Namely, the Néel temperature is 7.3 K at 5.3 GPa and becomes zero at 6.5 GPa in the diamond anvil cell experiment, although the Néel temperature is approximately zero at 5.5 GPa in the cubic anvil cell experiment. This might be due to the fact that pressure is inhomogeneously applied to the sample in the diamond anvil cell compared to the quasi-static pressure in the cubic anvil cell.

The inhomogeneous pressure presumably does not result in a uniform state of superconductivity in the entire sample, as noted for CeRh<sub>2</sub>Si<sub>2</sub> [18]. This is most likely the cause of the slow drop of the resistivity below  $T_{sc}$  and a non-zero resistivity of  $30 \mu\Omega$  cm even at 80 mK under 6.5 GPa, as shown in figure 6. Moreover, the wide superconducting pressure region from 4 to 10 GPa is also related to it. In other words, a true superconducting region might exist in a much narrower pressure region around  $P_c$  in which the heavy fermion state is formed.

In conclusion, we have done the experiment of the electrical resistivity under pressure for the antiferromagnet CeNiGe<sub>3</sub>. The electronic states of CeNiGe<sub>3</sub> are thus tuned by pressure



**Figure 7.** Temperature dependence of the upper critical field  $H_{c2}$  at three pressures in  $\text{CeNiGe}_3$ . Solid lines are guidelines.

from the Kondo state with antiferromagnetic ordering to the non-magnetic state (the valence fluctuating state), crossing the heavy fermion state at a critical pressure  $P_c \simeq 5.5$  GPa. Superconductivity has been discovered around  $P_c$ .

This work was financially supported by the Grant-in-Aid for Creative Scientific Research (15GS0123) and for Scientific Research of Priority Area from the Ministry of Education, Culture, Sports, Science and Technology of Japan.

## References

- [1] Ōnuki Y, Goto T and Kasuya T 1991 *Materials Science and Technology* vol 3A, ed K H J Buschow (Weinheim: VCH) p 545
- [2] Ōnuki Y, Inada Y, Ohkuni H, Settai R, Kimura N, Aoki H, Haga Y and Yamamoto E 2000 *Physica B* **280** 276
- [3] Doniach S 1977 *Valence Instabilities and Related Narrow-Band Phenomena* ed R D Parks (New York: Plenum) p 169
- [4] Aoki H, Uji S, Albessard A K and Ōnuki Y 1993 *Phys. Rev. Lett.* **71** 2110
- [5] Mathur N D, Grosche F M, Julian S R, Walker I R, Freye D M, Haselwimmer R K W and Lonzarich G G 1998 *Nature* **394** 39
- [6] Movshovich R, Graf T, Mandrus D, Thompson J D, Smith J L and Fisk Z 1996 *Phys. Rev. B* **53** 8241
- [7] Hegger H, Petrovic C, Moshopoulou E G, Hundley M F, Sarrao J L, Fisk Z and Thompson J D 2000 *Phys. Rev. Lett.* **84** 4986
- [8] Saxena S S, Agarwal P, Ahilan K, Grosche F M, Haselwimmer R K W, Steiner M J, Pugh E, Walker I R, Julian S R, Monthoux P, Lonzarich G G, Huxley A, Sheikin I, Braithwaite D and Fluquet J 2000 *Nature* **406** 587
- [9] Settai R, Araki S, Shishido H, Inada Y, Haga Y, Yamamoto E, Kobayashi T C, Tateiwa N and Ōnuki Y 2003 *J. Magn. Magn. Mater.* **262** 399
- [10] Salamakha P, Konyk M, Sologub O and Bodak O 1996 *J. Alloys Compounds* **236** 206
- [11] Durivault L, Bourée F, Chevalier B, André G, Weill F and Etourneau J 2002 *Appl. Phys. A* **74** S677
- [12] Durivault L, Bourée F, Chevalier B, André G, Weill F, Etourneau J, Martinez-Samper P, Rodrigo J, Suderow H and Vieira S 2003 *J. Phys.: Condens. Matter* **15** 77
- [13] Pikul A P, Kaczorowski D, Plackowski T, Czopnik A, Michor H, Bauer E, Hilscher G, Rogl P and Grin Y 2003 *Phys. Rev. B* **67** 224417
- [14] Yamada K, Yosida K and Hanzawa K 1984 *Prog. Theor. Phys.* **71** 450
- [15] Assmus W, Herrmann M, Rauchschalbe U, Riegel S, Lieke W, Spille H, Horn S, Weber G, Steglich F and Cordier G 1984 *Phys. Rev. Lett.* **52** 469
- [16] Araki S, Settai R, Inada Y, Ōnuki Y and Yamagami H 1999 *J. Phys. Soc. Japan* **68** 3334
- [17] Werthamer N R, Helfand E and Hohenberg P C 1965 *Phys. Rev.* **147** 295
- [18] Araki S, Nakashima M, Settai R, Kobayashi T C and Ōnuki Y 2002 *J. Phys.: Condens. Matter* **14** L377